A control problem approach to Coulomb's friction

D. Cerroni, L. Formaggia, A. Scotti *

Politecnico di Milano, P.za Leonardo Da Vinci 32, 20133 Milano, Italy

ARTICLE INFO

ABSTRACT

In this work we present a formulation of Coulomb's friction in a fractured elastic body as a PDE control problem where the observed quantity is the tangential stress across an internal interface, while the control parameter is the slip i.e. the displacement jump across the interface. The cost function aims at minimizing the norm of a non-linear and not everywhere differentiable complementarity function, written in terms of the tangential stress and the slip. The interesting point of this method is that gives rise to an iterative procedure where at each iteration we solve a problem with given slip at the interface, without resorting to the use of Lagrange multipliers. We carry out a formal derivation of the method, with some preliminary results, and a numerical experiment to verify the efficacy of the technique.

1. Introduction

The problem of modeling an elastic continuum in the presence of fractures that may slide has been the subject of intense study due to its application to many engineering and environmental problems, as well as to its mathematical interest. The most common models for frictional interfaces are Coulomb's, where the presence of sliding is related to the ratio between tangential and normal stresses at the fractured interface, and the Tresca one which is a simplified model where sliding occurs whenever the tangential stress overcome a fixed threshold. A seminal reference for this class of problems can be found in [1]. While Tresca problem gives rise to a classical variational inequality and several uniqueness results are available, the Coulomb's model gives rise to a pseudo-variational formulation which still poses several challenges at the analytical and numerical level.

On the analytical side, a review of recent results and some conditions for uniqueness of the Coulomb's friction model is contained in [2].

On the numerical level, several schemes have been presented for this class of problems, a few mentioned in the following. A first class of methods is based on the solution of an optimality system derived from a Lagrangian or augmented Lagrangian formulation using generalized or semi-smooth Newton schemes [3,4]. In [5] a primal–dual active set method is used on a dual-Lagrange formulation discretized using mortar techniques. The iterative scheme is applied to find the zero of a non-smooth complementary function for the friction condition which has some similarity with the one presented in this work. The technique has then been used in [6] to study contact mechanics in fractured poroelastic media. In [7] the reader may find a review of other fixed point techniques for both Tresca and Coulomb's friction problems.

A different class of techniques avoid the use of Lagrange multiplier by employing an extension of the Nitsche's method to contact problems. Nitsche's method, originally introduced as a way to impose Dirichlet conditions in elliptic problems, can be seen as a special consistent penalization technique. For an introduction to Nitsche's method for boundary conditions

---

* Corresponding author.
   E-mail addresses: daniele.cerroni@polimi.it (D. Cerroni), luca.formaggia@polimi.it (L. Formaggia), anna.scotti@polimi.it (A. Scotti).

and interface problems the reader may consult [8,9] and [10] for its extension to more general boundary conditions. In this class of methods we cite [11,12], where the friction interface conditions are treated as non-linear Robin-type conditions and enforced via an iterative scheme. A similar technique is used in [13], applied to earthquake rupture. Another interesting family of Nitsche's based schemes are those presented in [14–17], where a complementarity function for the contact problem is ingeniously exploited to derive a Nitsche's type penalization method. An overview is given in [18].

In this work we make a first attempt to a different formulation. For the sake of simplicity, we focus only on the friction condition, however the formulation can be extended to consider also normal contact. We recast the problem as a control problem where the control variable is the slip, i.e. the jump of tangential displacement across the fracture, while the observed variable is the tangential stress. We derive a complementary function which is different, yet equivalent, to that used in [5] or in [17]. We seek the zero of the complementary function by minimizing a cost functional, which eventually depends only on the slip. To this purpose we propose a simple gradient procedure which involves the solution of a primal and a dual problem governed by the same linear operator. One advantage of the technique, which does not make use of Lagrange multiplier, is that both primal and dual problem are differential problems where the slip, which is the jump of the displacement across the interface, is imposed on the whole fracture, thus a "standard" problem easily implementable using standard finite elements. In particular, we do not need to divide the fracture into two time dependent portions according to the magnitude of tangential stress to account for the fact that part of the fracture could slip, while the remaining part is stuck due to friction.

The scope of this work is to present the methodology and some preliminary numerical results, leaving its analysis to forthcoming work. We hope that this different point of view may open-up new insight about this interesting problem.

The paper is organized as follows. In Section 2 we recall the Coulomb's friction model and set up the notation used in Section 3, where we illustrate the control problem formulation. Section 4 is dedicated to the description of the numerical algorithm. Section 5 illustrates some numerical tests and it is followed by conclusions.

2. The model

We will consider a domain $\Omega \subset \mathbb{R}^2$, open, bounded and with Lipschitz boundary, cut by an internal planar (or C^1) interface Γ that represents the fracture. The fracture Γ partitions Ω into two disjoint subdomains, here indicated by Ω^+ and Ω^-, so that $\Omega = \text{int}(\Omega^+ \cup \Omega^- \cup \Gamma)$. We set $\Omega_\Gamma = \Omega \setminus \Gamma = \Omega^+ \cup \Omega^-$. We indicate with $\boldsymbol{n}_\Gamma$ the normal to Γ, conventionally oriented from Ω^+ to Ω^-, while $\boldsymbol{n}^+ = -\boldsymbol{n}^- = \boldsymbol{n}_\Gamma$ are the normal vectors oriented outwards with respect to the respective domain.

For a sufficiently regular scalar function $f : \Omega_\Gamma \to \mathbb{R}$ we define the average and jump across Γ as

$$\{f\} = \frac{f^+ + f^-}{2} \quad \text{and} \quad [\![f]\!] = f^+ - f^-$$

respectively, where, for $\mathbf{x} \in \Gamma$,

$$f^\pm(\mathbf{x}) = \lim_{\delta \to 0^+} f(\mathbf{x} + \delta \boldsymbol{n}_\Gamma^\pm).$$

This definition extends naturally to vector valued functions $\mathbf{f} : \Omega_\Gamma \to \mathbb{R}^2$, as

$$\{\mathbf{f} \cdot \boldsymbol{n}\} = \frac{\mathbf{f}^+ \cdot \boldsymbol{n}^+ + \mathbf{f}^- \cdot \boldsymbol{n}^-}{2} = \frac{[\![\mathbf{f} \cdot \boldsymbol{n}_\Gamma]\!]}{2},$$

and

$$[\![\mathbf{f} \cdot \boldsymbol{n}]\!] = \mathbf{f}^+ \cdot \boldsymbol{n}^+ - \mathbf{f}^- \cdot \boldsymbol{n}^- = 2\{\mathbf{f} \cdot \boldsymbol{n}_\Gamma\}.$$

In Ω_Γ, we indicate with $\mathbf{u}$ the displacement and with $\sigma = \sigma(\mathbf{u})$ the Cauchy stress tensor given by an elastic law of the form

$$\sigma(\mathbf{u}) = \lambda \, \text{tr}(\varepsilon(\mathbf{u})) + 2\mu \varepsilon(\mathbf{u}), \tag{1}$$

where, assuming linear elasticity, the strain tensor is given by the symmetric gradient of the displacement,

$$\varepsilon(\mathbf{u}) = \frac{1}{2}(\nabla \mathbf{u} + \nabla^T \mathbf{u}).$$

We have indicated with λ and μ the Lamè parameters, which we assume to be both positive and bounded in Ω_Γ.

We assume quasi-static mechanical balance, which means that we are facing the following differential equation

$$-\mathbf{div}\sigma(\mathbf{u}) = \mathbf{g} \quad \text{in } \Omega_\Gamma, \ t \geq 0. \tag{2}$$

The dependence on time may be due to the boundary conditions, for instance in the presence of incremental loads, or on the forcing term $\mathbf{g}$. The latter situation may arise in the simulation of poroelasticity problems when the mechanical part is split from the fluid flow computation, as in a fixed stress procedure [19]. We assume, however, that the evolution in time is sufficiently small to allow us neglecting the dynamic term in the mechanical balance.

The equations are supplemented by boundary conditions and interface conditions. In particular, a possible situation is

$$\begin{cases} \mathbf{u} = \mathbf{u}^\partial & \text{on } \partial\Omega_\mathbf{u} \\ \sigma(\mathbf{u}) \cdot \mathbf{n} = \boldsymbol{t}^\partial & \text{on } \partial\Omega_\sigma. \end{cases} \tag{3}$$

We assume that $|\partial\Omega_\mathbf{u} \cap \partial\Omega^+| > 0$ and $|\partial\Omega_\mathbf{u} \cap \partial\Omega^-| > 0$, which means that each portion of the domain has a part of the boundary where displacements are imposed.

Here, $\mathbf{u}^\partial$ and $\boldsymbol{t}^\partial$ are given data, possibly depending on time. Since we are using a quasi-static approach, we do not need initial conditions because the solution $\mathbf{u}(t)$ at each $t \geq 0$ is determined by the value of the boundary and forcing data at that time.

The system of equations (1), (2), (3) must be closed by suitable interface conditions on Γ. We first define the normal component of the stress on Γ and the corresponding vector as

$$\sigma_n = (\boldsymbol{\sigma} \cdot \boldsymbol{n}_\Gamma) \cdot \boldsymbol{n}_\Gamma, \quad \boldsymbol{\sigma}_n = \sigma_n \boldsymbol{n}_\Gamma.$$

The tangential stress on Γ is given instead by

$$\boldsymbol{\tau} = \boldsymbol{\sigma} \cdot \boldsymbol{n}_\Gamma - \boldsymbol{\sigma}_n. \tag{4}$$

Note that $\mathbf{u}$ may be discontinuous on Γ, consequently also normal and tangential stresses take a-priori two different values in correspondence to the plus and minus side of Γ.

Analogously, we define tangential and normal components of the displacement on Γ,

$$\mathbf{u}_n = u_n \cdot \boldsymbol{n}_\Gamma = (\mathbf{u} \cdot \boldsymbol{n}_\Gamma) \boldsymbol{n}_\Gamma, \quad \mathbf{u}_t = \mathbf{u} - \mathbf{u}_n, \tag{5}$$

and in the following we will use the suffixes n and t to indicate the normal and tangential component of a vector on Γ.

To describe the sliding conditions, we define

$$\mathcal{G} = |\{\boldsymbol{\tau}\}| + \mu_f \overline{\sigma}_n,$$

where, $|\cdot|$ indicates the Euclidean norm, $\mu_f > 0$ the friction coefficient, assumed constant, and $\overline{\sigma}_n$ a reference value of the normal component of the effective stress on the fracture, which may be taken as

$$\overline{\sigma}_n = \{\sigma_n\}. \tag{6}$$

We mention that in a poroelastic problem $\overline{\sigma}_n$ should account also for the component linked to fluid pressure. We also define on Γ the displacement velocity and its tangential component as

$$\dot{\mathbf{u}} = \frac{\partial \mathbf{u}}{\partial t} \quad \text{and} \quad \dot{\mathbf{u}}_t = \frac{\partial \mathbf{u}_t}{\partial t}. \tag{7}$$

We assume that the fracture may only act as a potentially sliding surface (yet the model may be readily extended to the case of possible aperture of the fracture). Consequently, at each time t the interface conditions on Γ may be expressed as

$$\begin{cases} [\![u_n]\!] &= 0, \\ [\![\sigma_n]\!] &= 0, \\ [\![\boldsymbol{\tau}]\!] &= \mathbf{0}, \end{cases} \tag{8}$$

complemented by the Coulomb's friction conditions [1]

$$\begin{cases} \{\boldsymbol{\tau}\} = \mathbf{0} & \text{if } \overline{\sigma}_n \geq 0; \\ \begin{cases} \mathcal{G} \leq 0, \\ \exists \beta \leq 0 \text{ s.t } [\![\dot{\mathbf{u}}_t]\!] = \beta\{\boldsymbol{\tau}\}, & \text{otherwise.} \\ \beta\mathcal{G} = 0. \end{cases} \end{cases} \tag{9}$$

Note that the balance of normal stresses implies that both σ_n and $\boldsymbol{\tau}$ are indeed continuous across Γ. However, also in view of the possible use of broken spaces in the numerical discretization, we will keep indicating the jumps for the normal and tangential components of the total stress.

Thanks to (8) at each time t we are able to identify two measurable portions of Γ, indicated by $\Gamma_D = \Gamma_D(t)$ and $\Gamma_D = \Gamma_D(t)$:

$$\begin{cases} \Gamma_D(t) = \overline{\{\mathbf{x} \in \Gamma : \mathcal{G}(\mathbf{x}) < 0\}}, \\ \Gamma_N(t) = \Gamma \setminus \Gamma_D(t), \end{cases} \tag{10}$$

as well as the convex set

$$\mathcal{K}_{-\mu_f \overline{\sigma}_n} = \{\mathbf{z} \in \mathbb{R}^d : |\mathbf{z}| - \mu_f \overline{\sigma}_n \leq 0\}.$$

We assume that, for any t, $\Gamma_N(t)$ is Lebesgue measurable and $\Gamma_N(t) \subset\subset \Gamma$ is a proper subset. This condition implies that $\text{supp}(\boldsymbol{\beta}) \subset\subset \Gamma$. In other words, we do not allow the interface to become completely broken.

2.1. The semi-discrete problem

It is useful to rewrite our problem at discrete times. To this purpose, we define the time step Δt and the sequence of time instants $t_n = n\Delta t$ for $n = 0, 1, \ldots$. At time $t = t_{n+1}$ we make the following approximation

$$[\![\dot{\mathbf{u}}_t(t_{n+1})]\!] = \frac{[\![\mathbf{u}_t(t_{n+1})]\!] - [\![\mathbf{u}_t(t_n)]\!]}{\Delta t} = \frac{\boldsymbol{\beta}(t_{n+1})}{\Delta t}, \tag{11}$$

where $\boldsymbol{\beta}$ now indicates the incremental displacement. We can then write our differential problem as: at each t_{n+1} find $\mathbf{u} = \mathbf{u}(t_{n+1})$ that satisfies

$$\begin{cases} -\mathbf{div}\sigma(\mathbf{u}) = \mathbf{g} & \text{in } \Omega_\Gamma, \\ \mathbf{u} = \mathbf{u}^\partial & \text{on } \partial\Omega_{\mathbf{u}} \\ \sigma(\mathbf{u}) \cdot \mathbf{n} = \mathbf{t}^\partial & \text{on } \partial\Omega_\sigma \\ [\![u_n]\!] = [\![\sigma_n]\!] = 0, & \text{on } \Gamma. \\ [\![\boldsymbol{\tau}]\!] = \mathbf{0}, & \text{on } \Gamma. \end{cases} \tag{12a}$$

and, on Γ

$$\begin{cases} \{\boldsymbol{\tau}\} = \mathbf{0} & \text{if } \overline{\sigma}_n \geq 0 \\ \begin{cases} \mathcal{G} \leq 0, \\ \exists \beta \leq 0 \text{ s.t } \boldsymbol{\beta} = \beta\{\boldsymbol{\tau}\}, & \text{otherwise} \\ \beta\mathcal{G} = 0. \end{cases} \end{cases} \tag{12b}$$

It is understood that all time dependent quantities are computed at time t_{n+1} and that now β depends also on the time step, while $\boldsymbol{\beta} = \boldsymbol{\beta}(t_{n+1})$ is as defined in (11). It can be noted that (12) is equivalent to a static Coulomb's friction problem.

2.2. Functional setting

We use the standard notation and norms for Lebesgue and Sobolev spaces for functions in $\Omega_\Gamma = \Omega \setminus \Gamma$. We define

$$L^2(\Omega_\Gamma) = \{v : \Omega_\Gamma \to \mathbb{R} : \int_\Omega v^2 < \infty\},$$

and we will use the same notation in boldface for vector functions whose components are in $L^2(\Omega_\Gamma)$. Note that since Γ is a set of zero 2-measure, a function in $L^2(\Omega_\Gamma)$ is naturally identified with a function in $L^2(\Omega)$. So, for u and v in $L^2(\Omega_\Gamma)$ we may write the L^2 inner product as

$$(u, v)_{L^2(\Omega_\Gamma)} = \int_{\Omega_\Gamma} uv = \int_\Omega uv,$$

and $\|u\|_{L^2(\Omega_\Gamma)} = \sqrt{(u, u)_{L^2(\Omega_\Gamma)}}$. The definition is readily extended to the space $\mathbf{L}^2(\Omega_\Gamma)$ of vector functions with components in $L^2(\Omega_\Gamma)$, where

$$(\mathbf{u}, \mathbf{v})_{\mathbf{L}^2(\Omega_\Gamma)} = \int_\Omega \mathbf{u} \cdot \mathbf{v}.$$

We also define

$$H^1(\Omega_\Gamma) = \{v \in L^2(\Omega_\Gamma) : \nabla v \in L^2(\Omega_\Gamma)\}, \tag{13}$$

with

$$(u, v)_{H^1(\Omega_\Gamma)} = (u, v)_{L_2(\Omega)} + \int_\Omega \nabla u \cdot \nabla v, \tag{14}$$

and

$$\|u\|^2_{H^1(\Omega_\Gamma)} = \sqrt{(u, u)_{H^1(\Omega_\Gamma)}}. \tag{15}$$

Analogous definition for vector valued functions:

$$\mathbf{H}^1(\Omega_\Gamma) = \{\mathbf{v} : \Omega_\Gamma \to \mathbb{R}^d : \mathbf{v} \in \mathbf{L}^2(\Omega_\Gamma) : \nabla\mathbf{v} \in \mathbf{L}^2(\Omega_\Gamma)\},$$

with the usual definition of inner product and norm.

The space $\mathbf{H}^1(\Omega_\Gamma)$ is a broken space, since its elements may be discontinuous across Γ. We thus define the following trace spaces

$$\boldsymbol{T}_t = \{\mathbf{v} : \Gamma \to \mathbb{R}^d : v_n = 0, \mathbf{v}_t \in [H^{1/2}(\Gamma)]^{d-1}\}, \quad T_n = H^{1/2}(\Gamma).$$

If $\mathbf{v} \in \boldsymbol{H}^1(\Omega_\Gamma)$ then $[\![\mathbf{v}_t]\!]$ and $\{\mathbf{v}_t\}$ are elements of $\boldsymbol{T}_t$, while $[\![v_n]\!]$ and $\{v_n\}$ are in T_n.

For the description of the variational formulation we consider, for the sake of simplicity, homogeneous Dirichlet boundary conditions on the whole $\partial\Omega$. The extension to more general settings may be carried out by standard means. We define the following subspaces

$$
\boldsymbol{V} = \{\mathbf{v} \in \boldsymbol{H}^1(\Omega_\Gamma) : \mathbf{v}|_{\partial\Omega} = \mathbf{0}\}, \quad \boldsymbol{V}_t = \{\mathbf{v} \in \boldsymbol{V} : [\![v_n]\!] = \mathbf{0}\},
$$
$$
\boldsymbol{V}_n = \{\mathbf{v} \in \boldsymbol{V} : [\![\mathbf{v}_t]\!] = \mathbf{0}\}, \qquad \boldsymbol{V}_0 = \boldsymbol{V}_t \cap \boldsymbol{V}_n,
\tag{16}
$$

and the following bilinear form and functional for functions in $\boldsymbol{H}^1(\Omega_\Gamma)$

$$
a(\mathbf{u}, \mathbf{v}) = \int_{\Omega_\Gamma} \boldsymbol{\sigma}(\mathbf{u}) : \boldsymbol{\varepsilon}(\mathbf{v}), \quad F(\mathbf{v}) = \int_{\Omega_\Gamma} \mathbf{g} \cdot \mathbf{v},
$$

where we have assumed $\mathbf{g} \in \boldsymbol{L}^2(\Omega)$.

It is well known [1] that problem (12) has a weak form which can be expressed as the following variational inequality:

Problem 2.1. Find $\mathbf{u} \in \boldsymbol{V}$ such that

$$
a(\mathbf{u}, \mathbf{v} - \mathbf{u}) + j(\mathbf{u}, \mathbf{v}) - j(\mathbf{u}, \mathbf{u}) \geq F(\mathbf{v} - \mathbf{u}), \quad \forall \mathbf{v} \in \boldsymbol{V}
\tag{17}
$$

where

$$
j(\mathbf{u}, \mathbf{v}) = \int_\Gamma \mu_f |\sigma_n(\mathbf{u})||\delta(\mathbf{v}_{t_\Gamma})|,
$$

with $\delta(\mathbf{v}) = [\![\mathbf{v}_{t_\Gamma}]\!] - [\![\mathbf{u}_t(t_n)]\!]$.

In the case of a Tresca problem, where σ_n is constant, the problem is well-posed [1], while in the more general case existence of solution has been demonstrated only if μ_f is sufficiently small [20], while non-uniqueness of solution has been shown in [21,22]. A recent uniqueness criterion, which still implies a sufficiently small μ_f, can be found in [2].

We want, however, to construct a different formulation for the problem and we start to derive its weak form in the case where $\boldsymbol{\beta} \in \boldsymbol{T}_t$ is a now given datum. More precisely, we consider the problem

$$
\begin{cases}
-\mathbf{div}\boldsymbol{\sigma}(\mathbf{u}) = \mathbf{g} & \text{in } \Omega, \\
\mathbf{u} = \mathbf{0} & \text{on } \partial\Omega, \\
[\![\mathbf{u}]\!] = [\![\mathbf{u}_t(t_n)]\!] + \boldsymbol{\beta} & \text{on } \Gamma, \\
[\![\boldsymbol{\sigma} \cdot \boldsymbol{n}_\Gamma]\!] = \mathbf{0} & \text{on } \Gamma.
\end{cases}
\tag{18}
$$

We proceed formally, by choosing a regular test function $\mathbf{v}$ which is zero on $\partial\Omega$ and applying the Stokes theorem, to get

$$
\langle -\mathbf{div}\boldsymbol{\sigma}(\mathbf{u}), \mathbf{v} \rangle = \int_{\Omega_\Gamma} \boldsymbol{\sigma}(\mathbf{u}) : \boldsymbol{\varepsilon}(\mathbf{v}) - \int_\Gamma [\![(\boldsymbol{\sigma}(\mathbf{u}) \cdot \boldsymbol{n}_\Gamma) \cdot \mathbf{v}]\!].
$$

Omitting the dependence on $\mathbf{u}$ we have

$$
-\int_\Gamma [\![(\boldsymbol{\sigma} \cdot \boldsymbol{n}_\Gamma) \cdot \mathbf{v}]\!] = -\int_\Gamma [\![\boldsymbol{\sigma} \cdot \boldsymbol{n}_\Gamma]\!] \cdot \{\mathbf{v}\} - \int_\Gamma \{\boldsymbol{\sigma} \cdot \boldsymbol{n}_\Gamma\} \cdot [\![\mathbf{v}]\!] =
$$
$$
-\int_\Gamma [\![\boldsymbol{\tau}]\!] \cdot \{\mathbf{v}_t\} - \int_\Gamma [\![\sigma_n]\!]\{v_n\} - \int_\Gamma \{\boldsymbol{\tau}\} \cdot [\![\mathbf{v}_t]\!] - \int_\Gamma \{\sigma_n\}[\![v_n]\!].
\tag{19}
$$

Using the previous relations and the interface conditions in (18), we may finally write that $\mathbf{u}$ satisfies

$$
\int_{\Omega_\Gamma} \boldsymbol{\sigma} : \boldsymbol{\varepsilon}(\mathbf{v}) - \int_\Gamma \{\boldsymbol{\tau}\} \cdot [\![\mathbf{v}_t]\!] - \int_\Gamma \{\sigma_n\}[\![v_n]\!] = \int_{\Omega_\Gamma} \rho \mathbf{g} \cdot \mathbf{v}.
\tag{20}
$$

for all test functions $\mathbf{v}$ that are zero on $\partial\Omega$.

We now consider the linear and bounded lifting operator $R_t : \boldsymbol{T}_t \to \boldsymbol{V}_t$ defined as

$$
\{R_t\mathbf{t}\} = \mathbf{t}, \ \exists c : \|R_t\mathbf{t}\|_{\boldsymbol{H}^1(\Omega_\Gamma)} \leq c\|\mathbf{t}\|_{\boldsymbol{T}_t}, \ \forall \mathbf{t} \in \boldsymbol{T}_t.
\tag{21}
$$

as well as $R_n : T_n \to \boldsymbol{V}_n$,

$$
\{R_n n \cdot \boldsymbol{n}_\Gamma\} = n, \ \exists c : \|R_n n\|_{\boldsymbol{H}^1(\Omega_\Gamma)} \leq c\|n\|_{T_n}, \ \forall n \in T_n.
\tag{22}
$$

From (20) we can infer the weak formulation of problem (18) as

Problem 2.2. Given $\mathbf{R}_\beta = R_t ([\![\mathbf{u}_t(t_n)]\!] + \boldsymbol{\beta})$, find $\mathbf{u} = \tilde{\mathbf{u}} + \mathbf{R}_\beta$ where $\tilde{\mathbf{u}} \in \boldsymbol{V}_0$ satisfies

$$
a(\tilde{\mathbf{u}}, \mathbf{v}) = F(\mathbf{v}) - a(\mathbf{R}_\beta, \mathbf{v}), \quad \forall \mathbf{v} \in \boldsymbol{V}_0.
\tag{23}
$$

Proposition 2.1. *Problem* 2.2 *is well posed and is equivalent to* (18).

Proof. Well posedness is obtained by noting that the restriction of $\tilde{\mathbf{u}}$ in $\Omega^{\pm}$ is in $\mathbf{H}_0^1(\Omega^{\pm})$. Consequently, we can apply Korn's Lemma to obtain that there exists and $\alpha > 0$ such that $a(\tilde{\mathbf{u}}, \tilde{\mathbf{u}}) \geq \alpha \|\tilde{\mathbf{u}}\|_{\mathbf{H}^1(\Omega_\Gamma)}^2$. The right hand side is a functional on $\mathbf{V}$ whose continuity derives from the continuity of F and a, as well as the boundedness of the lifting operator. Therefore, well posedness is provided by Lax–Milgram Lemma.

The equivalence of the problems may be ensured by observing that (20) reduces to (23) for functions in the chosen functional spaces, and that, by construction, $[\![\mathbf{u}_t]\!] = [\![\mathbf{u}_t(t_n)]\!] + \boldsymbol{\beta}$. By standard arguments, we may then infer that a solution of (18) satisfies Problem 2.2, while a sufficiently regular solution of 2.2 is a solution of (18). $\square$

We now note that having computed $\mathbf{u}$ we can recover the stresses on Γ by exploiting again (20) as follows,

$$\langle \{\boldsymbol{\tau}\}, \mathbf{t} \rangle = a(\mathbf{u}, R_t \mathbf{t}) - F(R_t \mathbf{t}), \ \forall \mathbf{t} \in \mathbf{T}_t, \tag{24a}$$

$$\langle \{\sigma_n\}, n \rangle = a(\mathbf{u}, R_n n) - F(R_n n), \ \forall n \in T_n, \tag{24b}$$

where $\langle \cdot, \cdot \rangle$ denotes the duality pairing between $\mathbf{T}_t$ and T_n with their respective dual. We have the following result:

Proposition 2.2. *For* $\mathbf{u} = \mathbf{u}(\boldsymbol{\beta})$ *solution of* (23), $\{\boldsymbol{\tau}(\boldsymbol{\beta})\} = \{\boldsymbol{\tau}(\mathbf{u}(\boldsymbol{\beta}))\}$, *computed using* (24a), *is an affine function of* $\boldsymbol{\beta}$, *and there exist constants* $0 < \underline{c}_t \leq \overline{c}_t$ *such that*

$$\underline{c}_t \|\boldsymbol{\beta}_1 - \boldsymbol{\beta}_2\| \leq \|\{\boldsymbol{\tau}(\boldsymbol{\beta}_1) - \boldsymbol{\tau}(\boldsymbol{\beta}_2)\}\| \leq \overline{c}_t \|\boldsymbol{\beta}_1 - \boldsymbol{\beta}_2\|.$$

Moreover, if $F = 0$ *in* (24a), $\{\boldsymbol{\tau}(\boldsymbol{\beta})\}$ *is a linear and continuous function and there exists a* $\underline{\alpha} > 0$ *such that*

$$\langle \{\boldsymbol{\tau}(\boldsymbol{\beta})\}, \boldsymbol{\beta} \rangle \geq \underline{\alpha} \|\boldsymbol{\beta}\|^2. \tag{25}$$

Proof. The proof is a consequence of the properties of the Dirichlet-to-Neumann operator (also called Steklov–Poincaré operator), and the coercivity of the bilinear form $a(\cdot, \cdot)$ on $\mathbf{V}$. For some details on the Dirichlet-to-Neumann operator the reader may consult [2] or [23]. The constants depend on the continuity and coercivity constants of the form a as well as the constants in the trace inequality. $\square$

2.3. The friction condition

We now reformulate the friction condition via a complementary function. First of all, for a $\rho \in \mathbb{R}$, we define the following:

- Projection operator: $\mathcal{P}_\rho : \mathbb{R}^d \to \mathcal{K}_\rho$,

$$\mathcal{P}_\rho(\mathbf{v}) = \begin{cases} \mathbf{0} & \text{if } \rho \leq 0, \\ \mathbf{v} & \text{if } |\mathbf{v}| < \rho, \\ \rho \mathbf{v} |\mathbf{v}|^{-1} & \text{otherwise.} \end{cases} \tag{26}$$

Note that we can use the more compact definition

$$\mathcal{P}_\rho(\mathbf{v}) = \mathbf{v} - \max\left(0, |\mathbf{v}| - \max(\rho, 0)\right) \mathbf{v} |\mathbf{v}|^{-1}. \tag{27}$$

- Augmented tangential stress $\mathbf{N} : \mathbb{R}^d \times \mathbb{R}^d \to \mathbb{R}^d$, for a $\gamma > 0$:

$$\mathbf{N} = \mathbf{N}(\mathbf{t}, \boldsymbol{v}) = \mathbf{t} - \gamma \boldsymbol{v}. \tag{28}$$

- Complementary function $\mathbf{D}_\rho : \mathbb{R}^d \times \mathbb{R}^d \to \mathbb{R}^d$:

$$\mathbf{D}_\rho(\mathbf{t}, \boldsymbol{v}) = \mathbf{t} - \mathcal{P}_\rho(\mathbf{N}(t, \boldsymbol{v})) = \mathbf{t} - \mathcal{P}_\rho(\mathbf{t} - \gamma \boldsymbol{v}). \tag{29}$$

In the following, for the sake of simplicity and convenience, we will sometime indicate with $\mathbf{N}(\boldsymbol{\beta})$ or $\mathbf{N}(\mathbf{u})$ the quantity $\mathbf{N}(\{\boldsymbol{\tau}(\mathbf{u})\}, \boldsymbol{\beta})$, where $\mathbf{u}$ is the solution of Eq. (18) for a given $\boldsymbol{\beta}$. The same applies for $\mathbf{D}_\rho(\boldsymbol{\beta})$ and $\mathbf{D}_\rho(\mathbf{u})$, which will sometimes be used to indicate $\mathbf{D}(\{\boldsymbol{\tau}(\mathbf{u})\}, \boldsymbol{\beta})$.

We define

$$\xi = \xi(\mathbf{t}, \boldsymbol{v}) = \max\left(0, 1 - \frac{\max(\rho, 0)}{|\mathbf{t} - \gamma \boldsymbol{v}|}\right) = \max\left(0, 1 - \frac{\max(\rho, 0)}{|\mathbf{N}(\mathbf{t}, \boldsymbol{v})|}\right). \tag{30}$$

We have that

$$\mathbf{D}_\rho(\mathbf{t}, \boldsymbol{v}) = (1 - \xi)\gamma \boldsymbol{v} + \xi \mathbf{t}. \tag{31}$$

Since, by construction, $0 \leq \xi < 1$ for all admissible values of ρ and of its arguments, $\mathbf{D}_\rho(\mathbf{u})$ is a convex combination of the tangential stress and the penalty term $\gamma \boldsymbol{\beta}$.

Now, for $\rho = -\mu_f \overline{\sigma}_n$, $\mathbf{v} = \boldsymbol{\beta}$, $\mathbf{t} = \mathbf{u}$ we can state the following result,

Proposition 2.3. *The friction condition* (12b) *is equivalent to the following equality*

$$\mathbf{D}_{-\mu_f \overline{\sigma}_n}(\mathbf{u}) = \{\boldsymbol{\tau}(\mathbf{u})\} - \mathcal{P}_{-\mu_f \overline{\sigma}_n}(\{\boldsymbol{\tau}(\mathbf{u})\} - \gamma \boldsymbol{\beta}) = 0 \tag{32}$$

on Γ.

Proof. In the case $\overline{\sigma}_n \leq 0$ (extensive case), clearly (32) implies $\{\boldsymbol{\tau}\} = \mathbf{0}$, as in (12b), and vice versa. We will then consider the case $\overline{\sigma}_n > 0$. Assume that (12b) is satisfied. If $\boldsymbol{\beta} = \mathbf{0}$ then $|\{\boldsymbol{\tau}\} - \gamma \boldsymbol{\beta}| = |\{\boldsymbol{\tau}\}| \leq -\mu_f \overline{\sigma}_n$, since $\mathcal{G} \leq 0$. This implies $\mathcal{P}_{-\mu_f \overline{\sigma}_n}(\mathbf{N}(\mathbf{u})) = \{\boldsymbol{\tau}(\mathbf{u})\}$, and thus $\mathbf{D}_{-\mu_f \overline{\sigma}_n}(\mathbf{u}) = \mathbf{0}$.

If instead $\boldsymbol{\beta} \neq \mathbf{0}$ then the second and the third condition in (12b) imply $|\{\boldsymbol{\tau}\}| = -\mu_f \overline{\sigma}_n = \mu_f |\overline{\sigma}_n|$ (since $\overline{\sigma}_n \leq 0$), and $\mathbf{N}(\mathbf{u}) = \{\boldsymbol{\tau}\} - \gamma \boldsymbol{\beta} = \{\boldsymbol{\tau}\} - \gamma \beta \{\boldsymbol{\tau}\} = (1 + \omega)\{\boldsymbol{\tau}\}$, with $\omega = -\gamma \beta > 0$. Thus, $|\mathbf{N}(\mathbf{u})| = |\{\boldsymbol{\tau}\} - \gamma \boldsymbol{\beta}| = (1 + \omega)|\{\boldsymbol{\tau}\}| = (1 + \omega)\mu_f |\overline{\sigma}_n| > \mu_f |\overline{\sigma}_n|$ and, consequently,

$$\mathcal{P}_{-\mu_f \overline{\sigma}_n}(\mathbf{N}(\mathbf{u})) = -\mu_f \overline{\sigma}_n \frac{\mathbf{N}(\mathbf{u})}{|\mathbf{N}(\mathbf{u})|} = \mu_f |\overline{\sigma}_n| \frac{\mathbf{N}(\mathbf{u})}{(1 + \omega)\mu_f |\overline{\sigma}_n|} =$$

$$\frac{1}{1 + \omega} \mathbf{N}(\mathbf{u}) = \frac{1 + \omega}{1 + \omega}\{\boldsymbol{\tau}(\mathbf{u})\} = \{\boldsymbol{\tau}(\mathbf{u})\}.$$

Therefore, $\mathbf{D}_{-\mu_f \overline{\sigma}_n}(\mathbf{u}) = \mathbf{0}$. We have then proved that (12b) leads to the satisfaction of (32).

Now, we prove the converse. We have two possible cases. The first is

$$|\mathbf{N}(\mathbf{u})| = |\{\boldsymbol{\tau}\} - \gamma \boldsymbol{\beta}| \leq -\mu_f \overline{\sigma}_n, \tag{33}$$

then $\mathbf{D}_{-\mu_f \overline{\sigma}_n}(\mathbf{u}) = \mathbf{0}$, which implies $\{\boldsymbol{\tau}\} - \{\boldsymbol{\tau}\} + \gamma \boldsymbol{\beta} = \gamma \boldsymbol{\beta} = \mathbf{0}$. Thus, $\boldsymbol{\beta} = 0$ and (33) gives $|\{\boldsymbol{\tau}\}| \leq -\mu_f \overline{\sigma}_n$, i.e. $\mathcal{G} \leq 0$, which is in agreement with (12b).

If we assume instead

$$|\mathbf{N}(\mathbf{u})| = |\{\boldsymbol{\tau}\} - \gamma \boldsymbol{\beta}| > -\mu_f \overline{\sigma}_n, \tag{34}$$

we have

$$\mathcal{P}_{-\mu_f \overline{\sigma}_n}(\mathbf{N}(\mathbf{u})) = -\mu_f \overline{\sigma}_n \frac{\mathbf{N}(\mathbf{u})}{|\mathbf{N}(\mathbf{u})|} = \frac{-\mu_f \overline{\sigma}_n}{|\{\boldsymbol{\tau}(\mathbf{u})\} - \gamma \boldsymbol{\beta}|} (\boldsymbol{\tau}(\mathbf{u}) - \gamma \boldsymbol{\beta}).$$

Consequently, $\mathbf{D}_{-\mu_f \overline{\sigma}_n}(\mathbf{u}) = \mathbf{0}$ implies

$$\{\boldsymbol{\tau}(\mathbf{u})\} + \frac{\mu_f \overline{\sigma}_n}{|\{\boldsymbol{\tau}(\mathbf{u})\} - \gamma \boldsymbol{\beta}|} (\boldsymbol{\tau}(\mathbf{u}) - \gamma \boldsymbol{\beta}) = \mathbf{0},$$

and, therefore,

$$\boldsymbol{\beta} = \frac{1}{\gamma} \left(\frac{|\{\boldsymbol{\tau}(\mathbf{u})\} - \gamma \boldsymbol{\beta}|}{\mu_f \overline{\sigma}_n} + 1 \right) \{\boldsymbol{\tau}(\mathbf{u})\}.$$

Since we have assumed $\overline{\sigma}_n < 0$, we can write

$$\boldsymbol{\beta} = \beta\{\boldsymbol{\tau}(\mathbf{u})\}, \quad \text{with } \beta = \frac{1}{\gamma} \left(1 - \frac{|\{\boldsymbol{\tau}(\mathbf{u})\} - \gamma \boldsymbol{\beta}|}{\mu_f |\overline{\sigma}_n|} \right) < 0, \tag{35}$$

since $|\{\boldsymbol{\tau}(\mathbf{u})\} - \gamma \boldsymbol{\beta}| > \mu_f |\overline{\sigma}_n|$. We have already found that

$$\{\boldsymbol{\tau}(\mathbf{u})\} = \frac{\mu_f |\overline{\sigma}_n|}{|\{\boldsymbol{\tau}(\mathbf{u})\} - \gamma \boldsymbol{\beta}|} (\{\boldsymbol{\tau}(\mathbf{u})\} - \gamma \boldsymbol{\beta}),$$

then, by taking the Euclidean norm on both sides, we get $|\{\boldsymbol{\tau}(\mathbf{u})\}| = \mu_f |\overline{\sigma}_n|$, by which $\mathcal{G}(\mathbf{u}) = 0$, and this completes the proof. $\square$

This interpretation opens up different possibility. The first, developed by Y. Renard, Chouly et al. [18,24] is to develop a Nitsche's formulation that exploits this condition. In this work we explore another possibility, described in the next section.

3. A control problem formulation

We set in the following $\rho = -\mu_f \overline{\sigma}_n$ and we indicate with $\langle \cdot, \cdot \rangle$ the duality pairing between $\boldsymbol{T}_t$ and its dual, while $(\cdot, \cdot)$ indicates the inner product in the relevant spaces.

To simplify the derivation, we consider approximate derivatives, in particular we assume that ρ is given, that is we ignore the variations with respect to ρ (which can however be accounted for at the price of a more complex derivation). This is justified by the fact that in the numerical procedure the problem will be solved as a succession of Tresca problems.

We consider $\boldsymbol{\beta} \in \boldsymbol{T}_t$ as our control variable, while $\{\boldsymbol{\tau}\} \in \boldsymbol{T}_t'$ is our observed variable. We assume that we can reconstruct $\mathbf{D}_\rho(\{\boldsymbol{\tau}\}, \boldsymbol{\beta})$ as an element of $\boldsymbol{T}_t$ by the use of the Ritz representation theorem. We employ a cost function given by the following regularized functional,

$$J(\boldsymbol{\tau}, \boldsymbol{\beta}) = \frac{1}{2}(\mathbf{D}_\rho(\boldsymbol{\tau}, \boldsymbol{\beta}), \mathbf{D}_\rho(\boldsymbol{\tau}, \boldsymbol{\beta})) + \frac{\zeta}{2}(\boldsymbol{\beta}, \boldsymbol{\beta}) = J_D(\boldsymbol{\tau}, \boldsymbol{\beta}) + \frac{\zeta}{2}\|\boldsymbol{\beta}\|_{L^2(\Gamma)}^2,$$

where $\zeta \geq 0$ is the Tikhonov regularization parameter. In the following we will set $j_D = |\mathbf{D}_\rho|^2$.

We proceed formally by defining the following Lagrangian $L : \boldsymbol{V}_t \times \boldsymbol{T}_t \times \boldsymbol{V}_t' \times \boldsymbol{T}' \to \mathbb{R}$

$$\begin{aligned}
L(\mathbf{w}, \boldsymbol{\gamma}; \mathbf{q}, \boldsymbol{\alpha}) = & J(\{\boldsymbol{\tau}(\mathbf{w})\}, \boldsymbol{\gamma}) + \\
& \langle [\![\mathbf{w}_t]\!] - [\![\mathbf{u}_t(t_n)]\!] - \boldsymbol{\gamma}, \boldsymbol{\alpha}\rangle + A(\mathbf{w}, \mathbf{q}) - F(\mathbf{q}) - \langle \{\boldsymbol{\tau}(\mathbf{w})\}, [\![\mathbf{q}]\!]\rangle,
\end{aligned} \tag{36}$$

and we seek $\mathbf{u}$, $\boldsymbol{\beta}$, $\mathbf{p}$ and $\boldsymbol{\lambda}$ stationary point of L: i.e.

$$L(\mathbf{u}, \boldsymbol{\beta}; \mathbf{p}, \boldsymbol{\lambda}) = \inf_{(\mathbf{w}, \boldsymbol{\gamma})} \sup_{(\mathbf{q}, \boldsymbol{\alpha})} L(\mathbf{w}, \boldsymbol{\gamma}; \mathbf{q}, \boldsymbol{\alpha}).$$

In the following we indicate with $\partial_{\mathbf{x}} L(\mathbf{u}, \boldsymbol{\beta}; \mathbf{p}, \boldsymbol{\lambda})[\mathbf{v}]$ the directional derivative of L w.r.t $\mathbf{x}$ at point $(\mathbf{u}, \boldsymbol{\beta}, \mathbf{p}, \boldsymbol{\lambda})$ along $\mathbf{v}$, and, for the sake of notation, we write $\mathbf{D}_\rho$ and J_D for $\mathbf{D}_\rho(\{\boldsymbol{\tau}(\mathbf{u})\}, \boldsymbol{\beta})$ and $J_D(\{\boldsymbol{\tau}(\mathbf{u})\}, \boldsymbol{\beta})$, respectively.

We recall that $\boldsymbol{\tau}(\mathbf{u})$ is an affine function, so

$$\partial_{\mathbf{u}}\{\boldsymbol{\tau}(\mathbf{u})\}[\mathbf{v}] = \{\boldsymbol{\tau}(\mathbf{v})\}, \ \forall \mathbf{v} \in \boldsymbol{V}_t, \tag{37}$$

while

$$\partial_{\boldsymbol{\tau}} J_D[\mathbf{t}] = \langle \partial_{\boldsymbol{\tau}} j_D, \mathbf{t}\rangle = \langle \mathbf{D}_\rho^T \partial_{\boldsymbol{\tau}} \mathbf{D}_\rho, \mathbf{t}\rangle, \ \forall \mathbf{t} \in \boldsymbol{T}_t, \tag{38}$$

and

$$\partial_{\boldsymbol{\beta}} J_D[\mathbf{t}] = \langle \partial_{\boldsymbol{\beta}} j_D, \mathbf{t}\rangle = \langle \partial_{\boldsymbol{\beta}} j_D, \mathbf{t}\rangle, \ \forall \mathbf{t} \in \boldsymbol{T}_t. \tag{39}$$

We have that the stationary point is characterized by setting to zero the various derivatives. This provides the building blocks of our procedure.

The primal problem. The primal problem can be obtained by setting

$$\begin{cases}
\partial_{\mathbf{p}} L(\mathbf{u}, \boldsymbol{\beta}; \mathbf{p}, \boldsymbol{\lambda})[\mathbf{v}] = a(\mathbf{u}, \mathbf{v}) - F(\mathbf{v}) - \langle \{\boldsymbol{\tau}(\mathbf{u})\}, [\![\mathbf{v}_t]\!]\rangle = 0, \ \forall \mathbf{v} \in \boldsymbol{V}_t, \\
\partial_{\boldsymbol{\lambda}} L(\mathbf{u}, \boldsymbol{\beta}; \mathbf{p}, \boldsymbol{\lambda})[\boldsymbol{\phi}] = \langle [\![\mathbf{u}_t]\!] - [\![\mathbf{u}_t(t_n)]\!] - \boldsymbol{\beta}, \boldsymbol{\phi}\rangle = 0, \ \forall \boldsymbol{\phi} \in \boldsymbol{T}_t'
\end{cases} \tag{40}$$

for all $\mathbf{v} \in \boldsymbol{V}_t$ and all $\boldsymbol{\phi} \in \boldsymbol{T}_t'$.

We can recognize that $\mathbf{u}$ is the solution of Problem 2.2. Indeed it is immediate to verify that the solution of Problem 2.2 satisfies (40). Conversely, if $\mathbf{u}$ satisfies (40), then the second equation tells us that $[\![\mathbf{u}_t]\!] = [\![\mathbf{u}_t(t_n)]\!] + \boldsymbol{\beta}$, and $\mathbf{u}$ can thus be written in the form $\mathbf{u} = \tilde{\mathbf{u}} + R_t([\![\mathbf{u}_t(t_n)]\!] + \boldsymbol{\beta})$, with $\tilde{\mathbf{u}} \in \boldsymbol{V}_0$ solution of (23).

The dual problem. Using (38) and (37) we can write

$$\begin{aligned}
\partial_{\mathbf{u}} L(\mathbf{u}, \boldsymbol{\beta}; \mathbf{p}, \boldsymbol{\lambda})[\mathbf{w}] &= \partial_{\boldsymbol{\tau}} J_D[\{\boldsymbol{\tau}(\mathbf{w})\}] + \langle \boldsymbol{\lambda}, [\![\mathbf{w}_t]\!]\rangle + a(\mathbf{w}, \mathbf{p}) - \langle \{\boldsymbol{\tau}(\mathbf{w})\}, [\![\mathbf{p}_t]\!]\rangle \\
&= \langle \partial_{\boldsymbol{\tau}} j_D, \{\boldsymbol{\tau}(\mathbf{w})\}\rangle + \langle \boldsymbol{\lambda}, [\![\mathbf{w}_t]\!]\rangle + a(\mathbf{w}, \mathbf{p}) - \langle \{\boldsymbol{\tau}(\mathbf{w})\}, [\![\mathbf{p}_t]\!]\rangle.
\end{aligned}$$

So the stationary point of the Lagrangian satisfies, by exploiting the symmetry of $a(\cdot, \cdot)$,

$$a(\mathbf{p}, \mathbf{w}) + \langle \partial_{\boldsymbol{\tau}} j_D - [\![\mathbf{p}_t]\!], \{\boldsymbol{\tau}(\mathbf{w})\}\rangle + \langle \boldsymbol{\lambda}, [\![\mathbf{w}_t]\!]\rangle = 0, \ \forall \mathbf{w} \in \boldsymbol{V}_t. \tag{41}$$

If we build the *dual solution* $\mathbf{p} \in \boldsymbol{V}_t$ such that $\mathbf{p} = \tilde{\mathbf{p}} + R_t(\partial_{\boldsymbol{\tau}} j_D)$, and $\tilde{\mathbf{p}} \in \boldsymbol{V}_0$ solution of

$$a(\tilde{\mathbf{p}}, \mathbf{w}) = a(R_t(\partial_{\boldsymbol{\tau}} j_D), \mathbf{w}), \ \forall \mathbf{w} \in \boldsymbol{V}_t, \tag{42}$$

we can note that expression (41) reduces to

$$a(\mathbf{p}, \mathbf{w}) + \langle \boldsymbol{\lambda}, [\![\mathbf{w}_t]\!]\rangle = 0, \ \forall \mathbf{w} \in \boldsymbol{V}_t. \tag{43}$$

On the other hand, from (24a) applied to the dual solution and choosing $\mathbf{t} = [\![\mathbf{w}_t]\!]$, we have

$$\langle \{\boldsymbol{\tau}(\mathbf{p})\}, [\![\mathbf{w}_t]\!]\rangle = a(\mathbf{p}, \mathbf{w}), \quad \forall \mathbf{w} \in \boldsymbol{V}_t.$$

Therefore, (43) implies $\boldsymbol{\lambda} = -\{\boldsymbol{\tau}(\mathbf{p})\}$.

If we now consider that

$$\partial_{\boldsymbol{\beta}} L(\mathbf{u}, \boldsymbol{\beta}; \mathbf{p}, \boldsymbol{\lambda})[\boldsymbol{\gamma}] = \langle \partial_{\boldsymbol{\beta}} j_D, \boldsymbol{\gamma}\rangle + \zeta(\boldsymbol{\beta}, \boldsymbol{\gamma}) - \langle \boldsymbol{\lambda}, \boldsymbol{\gamma}\rangle,$$

we have

$$\partial_\beta L(\mathbf{u}, \boldsymbol{\beta}; \mathbf{p}, \lambda)[\boldsymbol{\gamma}] = \langle \partial_\beta j_D, \boldsymbol{\gamma} \rangle + \langle \{\boldsymbol{\tau}(\mathbf{p})\}, \boldsymbol{\gamma} \rangle + \zeta(\boldsymbol{\beta}, \boldsymbol{\gamma}) =$$
$$\langle \partial_\beta j_D, \boldsymbol{\gamma} \rangle + a(\mathbf{p}, R_t \boldsymbol{\gamma}) + \zeta(\boldsymbol{\beta}, \boldsymbol{\gamma}) \tag{44}$$

being $\mathbf{p}$ the dual solution previously defined. Since, in general,

$$\partial_\beta L(\mathbf{u}, \boldsymbol{\beta}; \mathbf{p}, \lambda) = D_\beta J(\mathbf{u}(\boldsymbol{\beta}), \boldsymbol{\beta}), \tag{45}$$

the quantity at the right hand side of (44) may drive a gradient based optimization scheme.

We need to define the terms containing the derivatives of $\mathbf{D}_\rho$. We have

$$\partial_\tau j_D \in \begin{cases} \mathbf{D}_\rho & \text{if } \rho \le 0, \\ \xi \mathbf{D}_\rho + (1 - \xi) \dfrac{\mathbf{N} \cdot \mathbf{D}_\rho}{|\mathbf{N}|^2} \mathbf{N} & \text{if } 0 < \rho < |\mathbf{N}|, \\ \mathbf{0} & \text{if } \rho > |\mathbf{N}|, \end{cases} \tag{46}$$

and

$$\partial_\beta j_D \in \begin{cases} \mathbf{0} & \text{if } \rho \le 0, \\ \gamma(1 - \xi)\left(\mathbf{D}_\rho - \dfrac{\mathbf{N} \cdot \mathbf{D}_\rho}{|\mathbf{N}|^2} \mathbf{N} \right) & \text{if } 0 < \rho < |\mathbf{N}|, \\ \gamma \mathbf{D}_\rho & \text{if } \rho > |\mathbf{N}|. \end{cases} \tag{47}$$

The terms are expressed as a differential inclusion since they are not defined for $\rho = |\mathbf{N}|$, being discontinuous at that point unless $\mathbf{D} \cdot \mathbf{N} = 0$.

Proposition 3.1. *Let us consider $\zeta = 0$. Then $\mathbf{D}_\rho(\{\boldsymbol{\tau}\}(\mathbf{u}), \boldsymbol{\beta}) = \mathbf{0}$ is equivalent to $D_\beta J(\{\boldsymbol{\tau}\}(\mathbf{u}), \boldsymbol{\beta}) = 0$. So a stationary point of J_D satisfies the condition $\mathbf{D}_\rho = \mathbf{0}$.*

Proof. The first part of the equivalence is trivial: if $\mathbf{D}_\rho = 0$ then $\partial_\beta j_D = \partial_\tau J = \mathbf{0}$. Consequently, $\{\boldsymbol{\tau}(\mathbf{p})\} = \mathbf{0}$ and we can conclude that $D_\beta J = \mathbf{0}$.

Let now suppose that we are at a stationary point, i.e. $D_\beta J = \mathbf{0}$, then from (45) we have

$$\partial_\beta j_D + \{\boldsymbol{\tau}(\mathbf{p})\} = \mathbf{0} \text{ a.e. on } \Gamma. \tag{48}$$

We now exploit (25) to state that

$$\langle \{\boldsymbol{\tau}(\partial_\tau j_D)\}, \partial_\tau j_D \rangle = \langle \{\boldsymbol{\tau}(\mathbf{p}(\partial_\tau j_D))\}, \partial_\tau j_D \rangle \ge \underline{\alpha} \|\partial_\tau j_D\|^2,$$

for a $\underline{\alpha} > 0$.

Thus, in a stationary point,

$$0 = \langle \partial_\beta j_D + \{\boldsymbol{\tau}(\mathbf{p})\}, \partial_\tau j_D \rangle \ge \langle \partial_\beta j_D, \partial_\tau j_D \rangle + \underline{\alpha} \|\partial_\tau j_D\|^2.$$

Since it may be shown, using the definitions in (46) and (47), that $\langle \partial_\beta j_D, \partial_\tau j_D \rangle \ge 0$, we derive that $\|\partial_\tau j_D\|^2 \le 0$, thus necessarily $\|\partial_\tau j_D\| = 0$ a.e. This result implies $\|\{\boldsymbol{\tau}(\mathbf{p})\}\| = 0$, and, as a consequence of (48), also $\|\partial_\beta j_D\| = 0$. Using again (46) and (47), together with the previous results, we obtain

$$\gamma \|\mathbf{D}_\rho\| = \|\partial_\beta j_D + \gamma \partial_\tau j_D\| \le \|\partial_\beta j_D\| + \gamma \|\partial_\tau j_D\| = 0$$

by which we conclude that $\|\mathbf{D}_\rho\| = 0$. $\square$

4. The numerical algorithm

We here present a gradient-based iterative procedure that for a given $\mathbf{u}^{(0)}$ at time $t = 0$ solves at each time step the control problem to find the slip vector on the fracture that ensures the satisfaction of the friction condition. We here assume that the domain Ω is polyhedral and that Γ is piecewise planar, so that we can discretize the domain with a conforming grid $\mathcal{M}_h$ of elements K, such that $\cup K = \overline{\Omega}$. The mesh $\mathcal{M}_h$ can be partitioned into $\mathcal{M}_h^+$ and $\mathcal{M}_h^-$, which cover Ω^+ and Ω^-, respectively.

We assume that $\mathcal{M}_h$ is conforming also to the fracture, which means that we can identify on Γ a $d - 1$ dimensional grid Γ_h which satisfies

$$\Gamma_h = \Gamma_h^+ = \Gamma_h^- = \mathcal{M}_h \cap \Gamma.$$

The iterative procedure seeks at each time $t_n = n\Delta t$ an approximation $\mathbf{u}_h = \mathbf{u}_h^n \in \mathbf{V}_h \subset \mathbf{V}$, where $\mathbf{u}_h^n \simeq \mathbf{u}(t_n)$ and $\mathbf{V}_h$ is a generic finite element space. It means that a function $\mathbf{u}_h \in \mathbf{V}_h$ can be expressed as linear combination of finite element basis functions, as

$$\mathbf{u}_h(\mathbf{x}) = \sum_{i \in \mathcal{I}^+} u_i^+ \boldsymbol{\psi}_i^+(\mathbf{x}) + \sum_{i \in \mathcal{I}^-} u_i^- \boldsymbol{\psi}_i^-(\mathbf{x}) + \sum_{i^+ \in \mathcal{G}^+} u_{i^+}^+ \boldsymbol{\psi}_{i^+}^+(\mathbf{x}) \sum_{i^- \in \mathcal{G}^-} u_{i^-}^- \boldsymbol{\psi}_{i^-}^-(\mathbf{x}), \tag{49}$$

where $\mathcal{I}^\pm$ collect the indexes of the degrees of freedom for which $\mathrm{supp}(\boldsymbol{\psi}_i^\pm) \subset \Omega^\pm$, (we recall that $\Omega^\pm$ are open sets), while $\mathcal{I}^\pm$ those for which $\mathrm{supp}(\boldsymbol{\psi}^\pm) \cap \Gamma^\pm \neq \emptyset$. The scalars $u_i^\pm$ and $u_{i^\pm}^\pm$ are the degrees of freedom, i.e. the unknowns of our discrete problem. Clearly, the basis functions $\boldsymbol{\psi}_i^\pm$ span a subset of $\mathbf{V}_0$.

Since $\mathcal{M}_h$ is conformal to Γ we can approximate the trace space $\mathbf{T}_t$, for instance, as

$$\mathbf{T}_{t,h} = \{\mathbf{t}_h : \mathbf{t}_h = \{\mathbf{v}_{t,h}\}, \text{ for a } \mathbf{v}_h \in \mathbf{V}_h\},$$

where $\mathbf{v}_{t,h}$ indicates the tangential component of $\mathbf{v}_h$. Analogously for $T_{n,h}$, the approximating space of T_n. We note that for each index $i^+ \in \mathcal{G}_h^+$ there is a corresponding index $i^- \in \mathcal{G}_h^-$ so that $\boldsymbol{\psi}_{i^-}^-|_\Gamma = \boldsymbol{\psi}_{i^+}^+|_\Gamma$, and we set

$$\mathcal{G}_h = \{(i^+, i^-), \, i^+ \in \mathcal{G}_h^+, \, i^- \in \mathcal{G}_h^- \, : \, \boldsymbol{\psi}_{i^-}^-|_\Gamma = \boldsymbol{\psi}_{i^+}^+|_\Gamma\}.$$

4.1. The algebraic setting

We are now in the position of describing the algebraic setting for the solution of (23), and analogously for (42).

Following the decomposition (49) we can define $\mathbf{u}_{\Omega^\pm}$ as the vectors of the internal degrees of freedom appearing the first two terms of the sum, while $\mathbf{u}_{\Gamma^+}$ and $\mathbf{u}_{\Gamma^-}$ are the vectors of the dofs on the interface Γ that appear in the last two. Furthermore we indicate with $\boldsymbol{\Sigma}_h$ the vector containing the degrees of freedom for the reconstructed discrete normal stresses $\sigma(\mathbf{u}_h) \cdot \mathbf{n}_\Gamma$. Starting from the weak form (20) we may build the following linear system, where *we have not yet imposed the conditions on Γ*:

$$\begin{bmatrix} A_{\Omega^+\Omega^+} & \mathbf{0} & A_{\Omega^+\Gamma^+} & \mathbf{0} \\ \mathbf{0} & A_{\Omega^-\Omega^-} & \mathbf{0} & A_{\Omega^-\Gamma^-} \\ A_{\Gamma^+\Omega^+} & \mathbf{0} & A_{\Gamma^+\Gamma^+} & \mathbf{0} \\ \mathbf{0} & A_{\Gamma^-\Omega^-} & \mathbf{0} & A_{\Gamma^-\Gamma^-} \end{bmatrix} \begin{bmatrix} \mathbf{u}_{\Omega^+} \\ \mathbf{u}_{\Omega^-} \\ \mathbf{u}_{\Gamma^+} \\ \mathbf{u}_{\Gamma^-} \end{bmatrix} = \begin{bmatrix} \mathbf{f}_{\Omega^+} \\ \mathbf{f}_{\Omega^-} \\ \mathbf{f}_{\Gamma^+} + M\boldsymbol{\Sigma}_h \\ \mathbf{f}_{\Gamma^-} - M\boldsymbol{\Sigma}_h \end{bmatrix}.$$

Here, the various matrices indicated by A are the contributions to the standard stiffness matrix, while M is the mass matrix on Γ, which can be computed, since the discretization is conforming, as

$$M_{ij} = \frac{1}{2} \left(\int_{\Gamma^+} \boldsymbol{\psi}_{i^+} \cdot \boldsymbol{\psi}_{j^+} + \int_{\Gamma^-} \boldsymbol{\psi}_{i^-} \cdot \boldsymbol{\psi}_{j^-} \right).$$

We have the following relations,

$$\mathbf{u}_{\Gamma^+} = \{\mathbf{u}_h\} + \frac{1}{2}[\![\mathbf{u}_h]\!], \quad \mathbf{u}_{\Gamma^-} = \{\mathbf{u}_h\} - \frac{1}{2}[\![\mathbf{u}_h]\!], \tag{50}$$

where $\{\mathbf{u}_h\}$ and $[\![\mathbf{u}_h]\!]$ are the vectors whose components are $(u_{i^+}^+ + u_{i^-}^+)/2$ and $u_{i^+}^+ - u_{i^-}^+$, for $(i^+, i^-) \in \mathcal{G}_h$, respectively.

Thus, the previous system may be rewritten as

$$\begin{bmatrix} A_{\Omega^+\Omega^+} & \mathbf{0} & A_{\Omega^+\Gamma^+} & \frac{1}{2}A_{\Omega^+\Gamma^+} \\ \mathbf{0} & A_{\Omega^-\Omega^-} & A_{\Omega^-\Gamma^-} & -\frac{1}{2}A_{\Omega^-\Gamma^-} \\ A_{\Gamma^+\Omega^+} & \mathbf{0} & A_{\Gamma^+\Gamma^+} & \frac{1}{2}A_{\Gamma^+\Gamma^+} \\ \mathbf{0} & A_{\Gamma^-\Omega^-} & A_{\Gamma^-\Gamma^-} & -\frac{1}{2}A_{\Gamma^-\Gamma^-} \end{bmatrix} \begin{bmatrix} \mathbf{u}_{\Omega^+} \\ \mathbf{u}_{\Omega^-} \\ \{\mathbf{u}_h\} \\ [\![\mathbf{u}_h]\!] \end{bmatrix} = \begin{bmatrix} \mathbf{f}_{\Omega^+} \\ \mathbf{f}_{\Omega^-} \\ \mathbf{f}_{\Gamma^+} + M\boldsymbol{\Sigma}_h \\ \mathbf{f}_{\Gamma^-} - M\boldsymbol{\Sigma}_h \end{bmatrix}$$

We now replace the last two block-rows with their sum and difference, respectively. We further impose the condition $[\![\sigma(\mathbf{u}_h) \cdot \mathbf{n}_\Gamma]\!] = \mathbf{0}$ by setting $[\![\boldsymbol{\Sigma}_h]\!] = \mathbf{0}$. After a further division by 2 of the last block-row, we finally obtain

$$\begin{bmatrix} A_{\Omega^+\Omega^+} & \mathbf{0} & A_{\Omega^+\Gamma^+} & \frac{1}{2}A_{\Omega^+\Gamma^+} \\ \mathbf{0} & A_{\Omega^-\Omega^-} & A_{\Omega^-\Gamma^-} & -\frac{1}{2}A_{\Omega^-\Gamma^-} \\ A_{\Gamma^+\Omega^+} & A_{\Gamma^-\Omega^-} & A_\Gamma & \mathbf{0} \\ \frac{1}{2}A_{\Gamma^+\Omega^+} & -\frac{1}{2}A_{\Gamma^-\Omega^-} & \mathbf{0} & \frac{1}{2}A_\Gamma \end{bmatrix} \begin{bmatrix} \mathbf{u}_{\Omega^+} \\ \mathbf{u}_{\Omega^-} \\ \{\mathbf{u}_h\} \\ [\![\mathbf{u}_h]\!] \end{bmatrix} = \begin{bmatrix} \mathbf{f}_{\Omega^+} \\ \mathbf{f}_{\Omega^-} \\ \mathbf{f}_{\Gamma^+} + \mathbf{f}_{\Gamma^-} \\ \frac{1}{2}(\mathbf{f}_{\Gamma^+} - \mathbf{f}_{\Gamma^-}) + M\{\boldsymbol{\Sigma}_h\} \end{bmatrix}, \tag{51}$$

where we have exploited the fact that, being the mesh conforming, $A_{\Gamma^+\Gamma^+} = A_{\Gamma^-\Gamma^-}$ and we have set $A_\Gamma = \frac{1}{2}(A_{\Gamma^+\Gamma^+} + A_{\Gamma^-\Gamma^-}) = A_{\Gamma^+\Gamma^+} = A_{\Gamma^-\Gamma^-}$.

The imposition of $\llbracket \mathbf{u}_h \rrbracket = \boldsymbol{\beta}_h$, where $\boldsymbol{\beta}_h$ is the vector with the nodal values of $\boldsymbol{\beta}$ allows us to compute the actual unknowns $[\mathbf{u}_{\Omega+}, \mathbf{u}_{\Omega-}, \{\mathbf{u}_h\}]^T$ by solving the following reduced system,

$$
\begin{bmatrix}
A_{\Omega+\Omega+} & \mathbf{0} & A_{\Omega+\Gamma+} \\
\mathbf{0} & A_{\Omega-\Omega-} & A_{\Omega-\Gamma-} \\
A_{\Gamma+\Omega+} & A_{\Gamma-\Omega-} & A_\Gamma
\end{bmatrix}
\begin{bmatrix}
\mathbf{u}_{\Omega+} \\
\mathbf{u}_{\Omega-} \\
\{\mathbf{u}_h\}
\end{bmatrix}
=
\begin{bmatrix}
\mathbf{f}_{\Omega+} - \frac{1}{2}A_{\Omega+\Gamma+}\boldsymbol{\beta}_h \\
\mathbf{f}_{\Omega-} + \frac{1}{2}A_{\Omega-\Gamma-}\boldsymbol{\beta}_h \\
\mathbf{f}_{\Gamma+} + \mathbf{f}_{\Gamma-}
\end{bmatrix},
\tag{52}
$$

which is in fact the discretization of (23), and to reconstruct the degrees of freedom at the interface using (50), as

$$
\mathbf{u}_{\Gamma+} = \{\mathbf{u}_h\} + \frac{1}{2}\boldsymbol{\beta}_h, \quad \mathbf{u}_{\Gamma-} = \{\mathbf{u}_h\} - \frac{1}{2}\boldsymbol{\beta}_h.
$$

The terms indicated with $\mathbf{f}$ in (52) stem from the discretization of the forcing terms and of the possible lifting terms in the case of non-homogeneous Dirichlet boundary conditions.

The average normal stress on Γ may then be computed solving

$$
M\{\Sigma_h\} = \frac{1}{2}(\mathbf{f}_{\Gamma-} - \mathbf{f}_{\Gamma+}) + \frac{1}{2}A_{\Gamma+\Omega+}\mathbf{u}_{\Omega+} - \frac{1}{2}A_{\Gamma-\Omega-}\mathbf{u}_{\Omega-} + \frac{1}{2}A_\Gamma\boldsymbol{\beta}_h,
\tag{53}
$$

from which one can easily compute the normal and tangential components at each node, and thus the value of $\{\boldsymbol{\tau}_h\}$ and $\sigma_{n,h}$.

Since the problem is self-adjoint, the same matrix governs the finite element discretization of the dual problem (42), for which we adopt the same finite element space.

4.2. A steepest descent algorithm

At each time step $t_n \to t_{n+1}$ the algorithm reads as follows.
Set $\boldsymbol{\beta}_h^{(0)} = \mathbf{0}$ and, for $k = 0, 1, \ldots,$

1. Find $\mathbf{u}_h^{(k)}$ by solving (52), and compute the corresponding values of $\{\boldsymbol{\tau}\}_h^{(k)}$ and $\{\sigma_n\}_h^{(k)}$, using (53). We can then compute $\rho^{(k)} = -\mu_f(\overline{\sigma}_n)^{(k)}$, $\mathbf{D}_h^{(k)} = \mathbf{D}_{\rho^{(k)}}(\{\boldsymbol{\tau}_h\}(k), \boldsymbol{\beta}_h^{(k)})$ and the corresponding cost function $J^{(k)}$.
2. Compute the discrete dual solution $\mathbf{p}_h^{(k)} \in \boldsymbol{V}_h$ by solving (52) where all the terms indicated by $\boldsymbol{f}$ are set to zero and $\boldsymbol{\beta}_h = \partial_{\boldsymbol{\tau}}J_{D,h}^{(k)}$ is evaluated using (46).
3. For a given step size α_k compute $\boldsymbol{\beta}_h^{(k+1)}$ by solving

$$
\boldsymbol{\beta}_h^{(k+1)} = (1 - \alpha_k\zeta)\boldsymbol{\beta}_h^{(k)} - \alpha_k\left(\partial_{\boldsymbol{\beta}}\mathbf{j}_{D,h}^{(k)} + \{\boldsymbol{\tau}(\mathbf{p}_h^{(k)})\}\right),
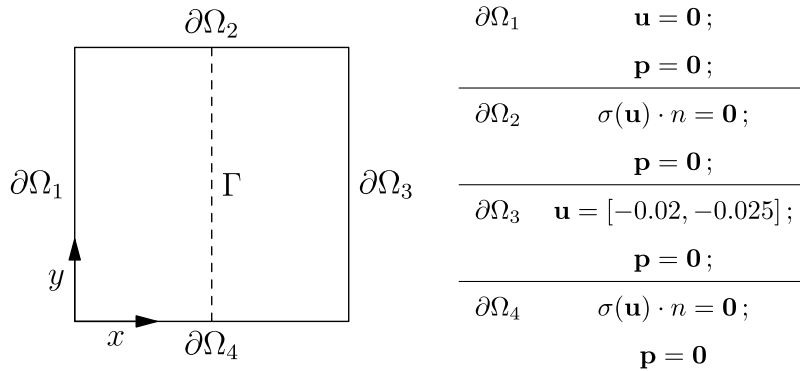\tag{54}
$$

where $\partial_{\boldsymbol{\beta}}\mathbf{j}_{D,h}^{(k)}$ is the vector with the components of the approximation of $\partial_{\boldsymbol{\beta}}\mathbf{j}_D$ at the mesh nodes and $\{\boldsymbol{\tau}(\mathbf{p}_h^{(k)})\}$ is obtained with the aid of (53).

The iteration continues until $\|\boldsymbol{\beta}^{(k+1)} - \boldsymbol{\beta}_h^{(k)}\|_{L^2(\Gamma)} \leq tol$, being tol a given tolerance.
The step α_k may be set by using a sufficient decrease rule as explained, for instance, in [25].

5. Numerical tests

In this section we investigate the performance of the new technique through numerical experiments. Numerical experiments are performed casting the problem in the Discontinuous Galerkin (DG) framework. This choice is mainly motivated by the natural handling of discontinuous fields by the DG method. The interested reader can find the formulation of the mechanical problem in the DG framework, together with the interior penalty method, in [26] and citations therein. Focusing on the set up of the numerical experiment, we consider a unit square domain with a central fracture (namely Γ) as shown in the left part of Fig. 1. According to the nomenclature shown in Fig. 1, we consider the domain clamped on $\partial\Omega_1$ and we impose a displacement $\mathbf{u} = [-0.02, -0.025]$ on $\partial\Omega_3$. Stress free conditions are considered in the remaining boundaries. Concerning the dual problem, homogeneous Dirichlet conditions are imposed on the whole boundary $\partial\Omega$. Focusing on the friction model we consider a limit friction coefficient $\mu_f = 0.4$ implying that when the slip tendency, defined as $ST = \boldsymbol{\tau}/\overline{\sigma}_n$ reaches the limit μ_f the fracture can slip. We will refer with $ST(\boldsymbol{\beta}_h^k)$ to the slip tendency obtained imposing the displacement jump $\llbracket \mathbf{u} \rrbracket = \boldsymbol{\beta}_h^k$ on Γ. The displacement imposed on the boundary $\partial\Omega_3$ is the only driving force of the primal problem and, if we impose a continuous displacement on the fracture, results in the continuous displacement field shown in Fig. 2. Such deformations lead to a slip tendency along the fracture that exceeds the friction limit and ignites the algorithm described in Section 4. Focusing on the steepest descent algorithm we consider, as reference case, $\gamma = 2$, $\zeta = 0$ and $\alpha_k = 0.0002$. In the left part of Fig. 3 the slip tendency ($ST(\boldsymbol{\beta}_h^k)$) along the fracture is shown after $k = 0$, 100 and 600 iterations. We can notice that the imposition of the $\boldsymbol{\beta}_h^k$, evaluated with Eq. (54), suddenly leads to a huge reduction of the excess of the ST with respect to the friction limit. In the right part of Fig. 2, the evolution of $\boldsymbol{\beta}_h^k$ at different iterations number is reported. In particular during the first iterations, curve $k = 0$

$\partial\Omega_1$	$\mathbf{u} = \mathbf{0}$;
	$\mathbf{p} = \mathbf{0}$;
$\partial\Omega_2$	$\sigma(\mathbf{u}) \cdot n = \mathbf{0}$;
	$\mathbf{p} = \mathbf{0}$;
$\partial\Omega_3$	$\mathbf{u} = [-0.02, -0.025]$;
	$\mathbf{p} = \mathbf{0}$;
$\partial\Omega_4$	$\sigma(\mathbf{u}) \cdot n = \mathbf{0}$;
	$\mathbf{p} = \mathbf{0}$

Fig. 1. On the left, a sketch of the domain and surface labeling. On the right, boundary conditions of the primal and adjoint problem.
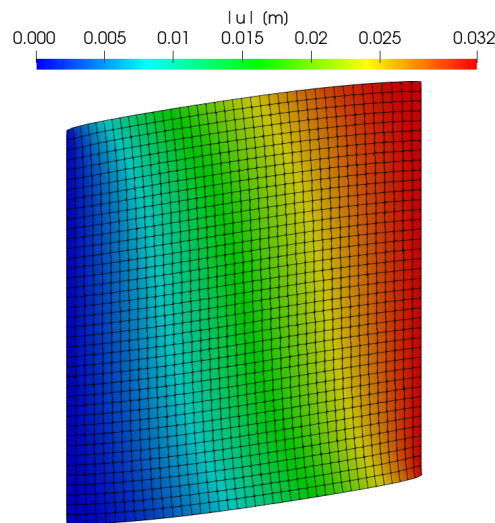

Fig. 2. Displacement field in the domain. The deformations are amplified of a factor 5 for visualization purposes; however we recall that we are working in the assumption of small displacements and small deformations.

and $k = 100$, we observe the formation of a negative peak of $\boldsymbol{\beta}_h^k$ located in correspondence of the maximum excess of $ST(\boldsymbol{\beta}_h^k)$ and, as a consequence, of the maximum value of ξ and $\mathbf{D}_{\rho^k}$. In this initial phase we also notice that $\boldsymbol{\beta}_h^k$ does not vanish where the fracture is not exceeding the friction limit and two smaller positive peaks form near the boundary between the active and the non active part of the fracture. Such effect is due to the nature of the dual problem in Ω^+ and Ω^- as we can see in Fig. 4 where the x and y components of the dual variable $\boldsymbol{p}$ are reported at the first iteration. We notice that, although the forcing term of the dual problem vanishes where the fracture does not exceed the friction limit, the corresponding solution $\boldsymbol{p}$ is not trivial in the inactive part. In particular the term $\partial_y \boldsymbol{p}_x$ reaches its maximum at the boundary between the active (the region outlined in white in Fig. 4) and inactive part of the fracture. Recalling that, for the chosen fracture geometry, $\{\boldsymbol{\tau}(\mathbf{p}_h^{(k)})\} \propto \{\partial_x \boldsymbol{p}_y + \partial_y \boldsymbol{p}_x\}$ we can now understand the cause for the formation of peaks of slip velocity in the inactive part of the fracture. It is interesting to notice that, after the initial drop of the $ST(\boldsymbol{\beta}_h^k)$ excess, the remaining iterations of the algorithm ($k = 600, 2000$) have indeed the effect of reducing, until it vanishes, $\boldsymbol{\beta}_h^k$ in the inactive part of the fracture as we can see in the right part of Fig. 2. We recall that $\boldsymbol{\beta}_h^{(k+1)}$ is obtained through Eq. (54) and in Fig. 5 we report $\{\boldsymbol{\tau}(\mathbf{p}_h^{(k)})\}$ and $\partial_{\boldsymbol{\beta}} \mathbf{j}_{D,h}^{(k)}$ at different iterations. We notice that during the first iterations $\{\boldsymbol{\tau}(\mathbf{p}_h^{(k)})\}$ is predominant, resulting in the initial ST reduction. After this initial phase the term $\partial_{\boldsymbol{\beta}} \mathbf{j}_{D,h}^{(k)}$, that takes into account also the penalization of $\boldsymbol{\beta}_h$ in the inactive part of the fracture, builds up driving the reduction of the positive, unphysical, peaks of $\boldsymbol{\beta}_h$.

To test the sensitivity of the method to parameters we performed the same numerical experiment using different γ so that its effect on the algorithm can be investigated. In Fig. 6 we show the $ST(\boldsymbol{\beta}_h)$, after 600 algorithm iterations, obtained with $\gamma = 0.5, 1, 2$ and 4. We notice that increasing values of γ reduce the accuracy in the fulfillment of the constraint μ_f on ST. In Fig. 7 we show $\boldsymbol{\beta}_h^k$ at $k = 100$ and $k = 600$ on the left and right part, respectively. We observe that increasing γ leads to a faster reduction of $\boldsymbol{\beta}_h^k$ in the inactive part of fracture. Comparing $\boldsymbol{\beta}_h^k$ (Fig. 7) and $ST(\boldsymbol{\beta}_h^k)$ (Fig. 6) at different k
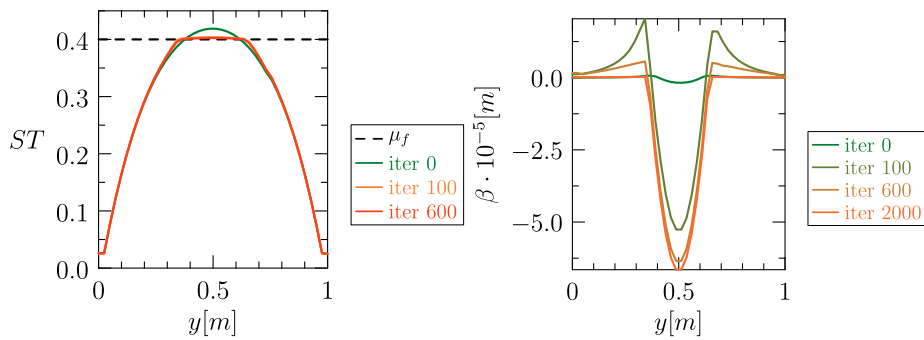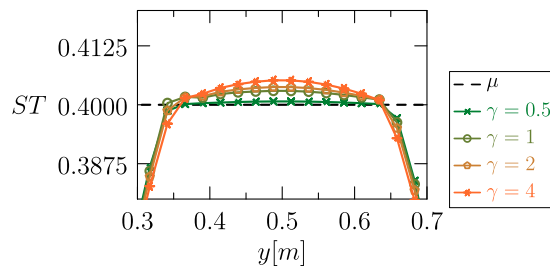
Fig. 3. Slip tendency, on the left, and β on the right along the fracture Γ at different iterations.
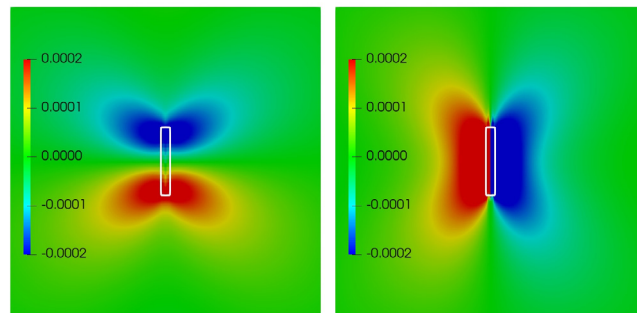
Fig. 4. Dual problem solution at the first iteration. x and y component on the left and right, respectively. The white region outlines the active part of the fracture.
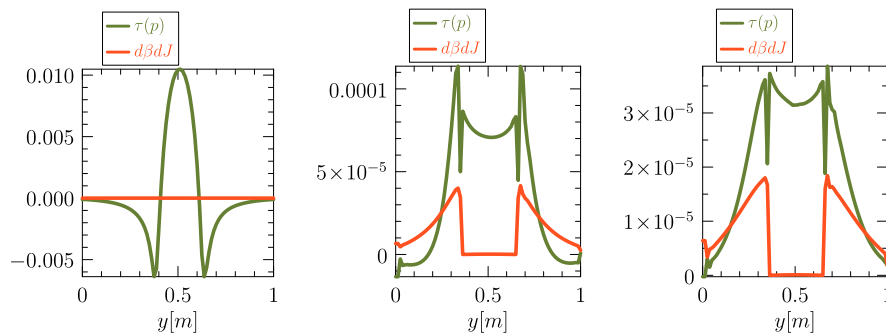
Fig. 5. Gradient components $\{\boldsymbol{\tau}(\mathbf{p}_h^{(k)})\}$ and $\partial_{\boldsymbol{\beta}}\mathbf{j}_{D,h}^{(k)}$ at different iterations from left to right $k = 0$, 300 and 800.

Fig. 6. Final ST ($k = 600$) using different Γ.

we notice that, from an empirical point of view, the higher the choice of γ the fewer iterations are needed to compute a consistent $\boldsymbol{\beta}_h$ that vanishes in the inactive part of the fracture. On the other hand, the higher the magnitude of γ the
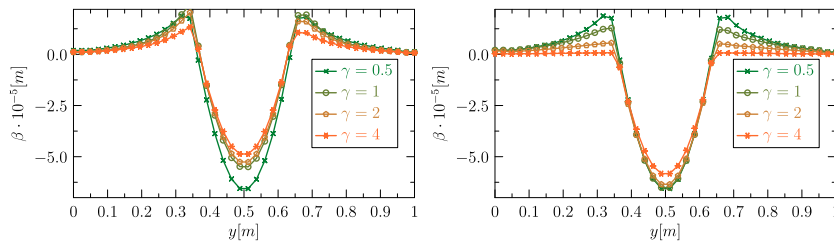
Fig. 7. β^k obtained with different γ at $k = 100$ and $k = 600$, on the left and right sides, respectively.
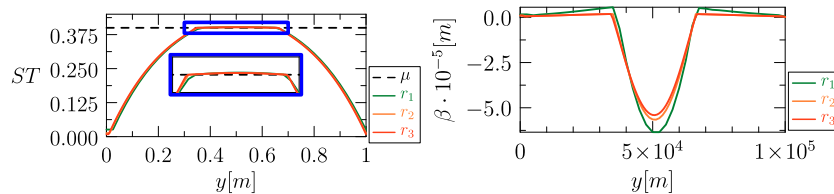

Fig. 8. Final slip tendency on the left, and β on the right, obtained for different mesh refinement.

lower the accuracy at which $ST(\boldsymbol{\beta}_h)$ fulfills the constraint imposed by the limit friction μ_f. Finally we investigate the effect of the characteristic grid size in the case $\gamma = 2$. In Fig. 8 we report the $ST(\boldsymbol{\beta}_h^k)$ and β_h^k, for $k = 600$, on the left and right part, respectively. We can notice that while the final ST is not influenced by the refinement of the grid, the final profile of β_h^k (at $k = 600$) varies with the refinement converging to an asymptotic value.

6. Conclusions

We have presented a technique based on control theory of PDEs to impose Coulomb friction condition along the interface of a fractured material. In this control problem the control variable is the slip along the fracture, while the observed variable is the tangential stress, which should not exceed the limit Coulomb's friction. The cost function aims at setting to zero a non-linear complementary function.

The resulting problem can be solved by an iterative procedure where, at each iteration, the slip along the fracture is imposed, with no need to introduce Lagrange multipliers. The matrix governing the primal and dual problem associated with the minimization procedure does not change during the iterations, and is the same matrix in the case of self-adjoint problems as the one considered here. This contrasts with other techniques where the matrix coefficients vary during the iterations, due to the nature of the frictional interface, where a point can transition from stuck to slipping, and vice-versa, in time and during the iterations within the same time step.

We have here derived the model in a rather formal way, a more thorough analysis of its properties will be subject of further work. Also, the numerical minimization algorithm we have used is rather basic and not yet optimized. Indeed, the procedure could be made more efficient for instance with a dynamic choice of the step length. However, the main objective of this work was to show that the proposed methodology is applicable and converges to a physically sound solution. The tests we have performed support the theoretical findings. More advanced (and efficient) algorithms such as quasi-Newton schemes like BFGS, or other acceleration techniques, may be implemented and will be tested in the future.

The main objective of this paper was indeed mainly to present the derivation of this original method in some detail, and justify it by some numerical experiments. We think that it may give a different insight on the numerical solution of Coulomb friction problems.

References

[1] N. Kikuchi, J.T. Oden, Contact Probelms in Elasticity: A Study of Variational Inequalities and Finite Element Methods, SIAM, 1988, p. 495.
[2] Yves Renard, A uniqueness criterion for the Signorini problem with Coulomb friction, SIAM J. Numer. Anal. 38 (2) (2006) 452−-467.
[3] P. Alart, A. Curnier, A mixed formulation for frictional contact problems prone to Newton like solution methods, Comput. Methods Appl. Mech. Engrg. 92 (3) (1991) 353–375.
[4] Yves Renard, Generalized Newton's methods for the approximation and resolution of frictional contact problems in elasticity, Comput. Methods Appl. Mech. Engrg. 256 (2013) 38–55.
[5] S. Hüeber, G. Stadler, B. Wohlmuth, A primal-dual active set algorithm for three-dimensional contact problems with Coulomb friction, SIAM J. Sci. Comput. 30 (2) (2008) 572–596.
[6] Runar L. Berge, Inga Berre, Eirik Keilegavlen, Jan M. Nordbotten, Barbara Wohlmuth, Finite volume discretization for poroelastic media with fractures modeled by contact mechanics, Internat. J. Numer. Methods Engrg. 121 (4) (2020) 644–663.
[7] Patrick Laborde, Yves Renard, Fixed point strategies for elastostatic frictional contact problems, Math. Methods Appl. Sci. 31 (March) (2008) 415–441.

[8] Anita Hansbo, Peter Hansbo, An unfitted finite element method, based on Nitsche's method, for elliptic interface problems, Comput. Methods Appl. Mech. Engrg. 191 (47–48) (2002) 5537–5552.

[9] Peter Hansbo, Nitsche's method for interface problems in computational mechanics, GAMM-Mitt. 28 (2) (2005) 183–206.

[10] Mika Juntunen, Rolf Stenberg, Nitsche's method for general boundary conditions, Math. Comput. 78 (267) (2009) 1353–1374.

[11] Chandrasekhar Annavarapu, Martin Hautefeuille, John E. Dolbow, A robust Nitsche's formulation for interface problems, Comput. Methods Appl. Mech. Engrg. 225–228 (2012) 44–54.

[12] Chandrasekhar Annavarapu, Martin Hautefeuille, John E. Dolbow, A Nitsche stabilized finite element method for frictional sliding on embedded interfaces. Part I: Single interface, Comput. Methods Appl. Mech. Engrg. 268 (2014) 417–436.

[13] E.T. Coon, B.E. Shaw, M. Spiegelman, A Nitsche-extended finite element method for earthquake rupture on complex fault systems, Comput. Methods Appl. Mech. Engrg. 200 (41–44) (2011) 2859–2870.

[14] Franz Chouly, Patrick Hild, A Nitsche-based method for unilateral contact problems: numerical analysis, SIAM J. Numer. Anal. 51 (2) (2013) 1295–1307.

[15] Franz Chouly, Patrick Hild, Yves Renard, A Nitsche finite element method for dynamic contact: 1. Space semi-discretization and time-marching schemes, ESAIM Math. Model. Numer. Anal. 49 (2) (2015) 481–502.

[16] Franz Chouly, An adaptation of Nitsche's method to the Tresca friction problem, J. Math. Anal. Appl. 411 (1) (2014) 329–339.

[17] Franz Chouly, Patrick Hild, Vanessa Lleras, Yves Renard, Nitsche-based finite element method for contact with Coulomb friction, in: Florin Adrian Radu, Kundan Kumar, Inga Berre, Jan Martin Nordbotten, Iuliu Sorin Pop (Eds.), Numerical Mathematics and Advanced Applications. ENUMATH 2017, in: Lecture Notes in Computational Science and Engineering, vol. 126, Springer International Publishing, Cham, 2019, pp. 839–847.

[18] Franz Chouly, Mathieu Fabre, Patrick Hild, Rabii Mlika, Jérôme Pousin, Yves Renard, An overview of recent results on Nitsche's method for contact problems, in: Stéphane P.A. Bordas, Erik Burman, Mats G. Larson, Maxim A. Olshanskii (Eds.), Geometrically Unfitted Finite Element Methods and Applications, Springer International Publishing, Cham, 2017, pp. 93–141.

[19] Birendra Jha, Ruben Juanes, Coupled multiphase flow and poromechanics: a computational model of pore pressure effects on fault slip and earthquake triggering, Water Resour. Res. 50 (5) (2014) 3776–3808.

[20] Jindrich Necas, Jirí Jarusek, Jaroslav Haslinger, On the solution of variational inequality to the Signorini problem with small friction, Boll. Unione Mat. Ital. 17-B (1980) 796–811.

[21] Patrick Hild, Non-unique slipping in the Coulomb friction model in two-dimensional linear elasticity, Q. J. Mech. Appl. Math. 57 (2) (2004) 225–235.

[22] Patrick Hild, Solution multiplicity and stick configurations in continuous and finite element friction problems, Comput. Methods Appl. Mech. Engrg. 196 (1–3) (2006) 57–65.

[23] Alfio Quarteroni, Alberto Valli, Domain Decomposition Methods for Partial Differential Equations, Oxford University Press, 1999.

[24] Franz Chouly, Patrick Hild, Vanessa Lleras, Yves Renard, Nitsche-based finite element method for contact with Coulomb friction, in: Florin Adrian Radu, Kundan Kumar, Inga Berre, Jan Martin Nordbotten, Iuliu Sorin Pop (Eds.), Numerical Mathematics and Advanced Applications ENUMATH 2017, Springer International Publishing, Cham, 2019, pp. 839–847.

[25] J. Nocedal, S. Wright, Numerical Optimization, Springer-Verlag GmbH, 2006.

[26] Douglas N Arnold, Franco Brezzi, Bernardo Cockburn, Donatella Marini, Discontinuous Galerkin methods for elliptic problems, in: Discontinuous Galerkin Methods, Springer, 2000, pp. 89–101.